Effect of perpendicular uniaxial anisotropy on the annihilation fields of magnetic vortices

E. R. P. Novais,[1] S. Allende,[2,3] D. Altbir,[3] P. Landeros,[4] F. Garcia,[5,a)] and A. P. Guimarães[1]
[1]*Centro Brasileiro de Pesquisas Físicas, Rio de Janeiro 22290-180, RJ, Brazil*
[2]*Departamento de Ciencias Físicas, Universidad Andrés Bello, Avenida República 220, Santiago 837-0134, Chile*
[3]*Departamento de Física, Universidad de Santiago de Chile and CEDENNA, Avda. Ecuador 3493, Santiago, Chile*
[4]*Departamento de Física, Universidad Técnica Federico Santa María, Avenida España 1680, Valparaíso, Chile*
[5]*Laboratório Nacional de Luz Síncrotron, Campinas 13083-970, SP, Brazil*

(Received 9 July 2013; accepted 25 September 2013; published online 16 October 2013)

The magnetization reversal in several nanoscopic systems is driven by the nucleation and propagation of a vortex structure that is very sensitive to the application of a magnetic field or a spin polarized current. In particular in a dot, the vortex profile is strongly affected by anisotropy, however, its role on the core behavior has not been clarified. In the present work, we investigate the influence of a perpendicular anisotropy on the annihilation and shape of magnetic vortex cores in permalloy disks. We used both micromagnetic simulations with the OOMMF code, and the analytical rigid core model that assumes that the shape of the core does not change during the hysteresis cycle. Under both approaches, the annihilation field decreases with increasing perpendicular anisotropy for almost all the structures investigated. Also a deformation of the vortex core profile is evidenced from the micromagnetic simulations, for larger anisotropy and/or dot thickness. For every dot thickness, this change does not depend on the dot radius, but on the relative distance of the core from the center of the dot. © *2013 AIP Publishing LLC*. [http://dx.doi.org/10.1063/1.4824803]

I. INTRODUCTION

Among the nano- and mesoscopic magnetic structures that have attracted the attention of researchers in recent years stand out those that exhibit a vortex, since this state presents both interesting physical properties and a high potential for applications.[1–6] Magnetic vortices in nanodots are characterized by in-plane magnetic moments curling around a core where the magnetization points out-of-plane. Two main features are defined in a vortex; the circulation, i.e., the sense of the magnetization curling, being -1 $(+1)$ for clockwise (counterclockwise) rotation direction, and the polarity defined by the direction of the core magnetization denoted by $p = +1$ (-1) for upward (downward) direction. The core profile $m_z(r)$ (the z component of the unit magnetization) of a vortex in equilibrium is cylindrically symmetric, usually approximated by a Gaussian curve surrounded by a small dip (see Fig. 1).[1,7]

A vortex is the ground state of different nanodots with regular shapes such as ellipses, squares, spheres, caps, and disks, with dimensions ranging from 50 nanometers to a few microns, with some tens of nanometers thickness.[8–14] While an external in-plane magnetic field that increases continuously from zero is applied to a disk exhibiting a vortex, its core propagates perpendicularly to the field direction, until its center reaches the disk edge. The field corresponding to this limiting situation, i.e., a field that expels the vortex core, is known as the annihilation field. Further increases of the magnetic field will expel the vortex from the disk, and the saturated state will eventually be reached. On the other hand, when starting from a fully saturated state, by decreasing the field to a certain critical value (commonly referred in the literature as the nucleation field) the vortex will be formed. The knowledge and control of the magnitude of these fields is a key issue for several applications considering the manipulation of magnetic vortices, such as nonvolatile magnetic memory devices, or high-resolution magnetic field sensors.[15–17]

The vortex core nucleation and annihilation processes have been discussed by several authors[18–23] and, in particular, the influence of extrinsic properties on the annihilation field has been taken into account. Wu *et al.*[24] investigated the role of geometrical asymmetries, finding that the annihilation of the vortex depends strongly on the asymmetry. The effect of the shape asymmetry has also been studied by Dumas *et al.*[25] by measuring the angular dependence of the annihilation field. Mihajlović *et al.*[26] have shown that temperature also affects the reversal mechanism and the vortex annihilation field, while experiments by Davis *et al.*[27] suggest that the nucleation and annihilation fields depend on the magnetic field sweep rate.

These processes have been also examined from the theoretical point of view, within the framework proposed by Guslienko *et al.*[20] This model approximates the core as a

a)Present address: Centro Brasileiro de Pesquisas Físicas, 22290-180 Rio de Janeiro, RJ, Brazil.

magnetization distribution whose profile does not change during the reversal process.

Some important properties of the vortices, such as the core size and some dynamic features, can be tailored introducing a uniaxial perpendicular magnetic anisotropy, as has been recently shown.[17,28] In this case, as the perpendicular anisotropy increases, important deviations from the equilibrium vortex core profile and from the canonical magnetic vortex configuration result. Beyond a critical value of the anisotropy (K_z^{crit}), a vortex is no longer observed and a skyrmion appears (e.g., Fert *et al.*[29]). The latter has been found in experiments with BFeCoSi[30] and, more relevant to the present study, also apparent in experiments with Co/Pt disks[17] and simulations.[14,17] In spite of the large number of works focused on magnetic vortices, the core deformation has not been systematically analyzed.

The aim of this paper is to obtain a better understanding of the vortex annihilation process in magnetic dots. For this purpose, we have compared the description using the rigid vortex analytical model to results obtained with micromagnetic simulations. In order to explore the effect of the perpendicular anisotropy on the vortex core properties, we have introduced an anisotropic term in both the analytical expressions and the numerical simulations. This procedure allows us to determine the limits of validity of the rigid vortex model. We also characterized the vortex core deformations that are present in some simulations.

The paper is organized as follows: after the "Introduction" we describe how we perform our micromagnetic simulations that lead us to study the annihilation fields extracted from the hysteresis curves of disks with various sizes (Sec. II). Analytical calculations are presented in Sec. III, with the inclusion of anisotropy terms into the rigid vortex model. The results are contained in Sec. IV, and finally, in Sec. V, we summarize and draw conclusions.

II. NUMERICAL SIMULATIONS

We focus on isolated magnetic nanodots with thickness L varying between 10 and 30 nm, and diameters D from 100 to 1000 nm, using micromagnetic simulations[14,31] with the OOMMF code.[32] We obtained the hysteresis loops of several nanodots including a uniaxial perpendicular anisotropy term, K_z, ranging from 0 to 300 kJ/m^3. We used a stiffness constant $A = 13 \times 10^{-12}$ J/m and a saturation magnetization $M_s = 860 \times 10^3$ A/m, both the standard values for bulk permalloy, and a cell size of $5 \times 5 \times 5$ nm^3. The maximum anisotropies used in this work that allow the dots to exhibit a magnetic vortex are $K_z^{max} = 300$, 225, and 165 kJ/m^3 for the thicknesses $L = 10$, 20, and 30 nm, respectively. For larger anisotropies, a skyrmion structure is observed, and perpendicular magnetization appears on the rim of the disk. For this reason in all our calculations, the anisotropy constant value was chosen such that the magnetic configuration at zero external applied field is a vortex configuration, as shown in Fig. 1.

In our simulations, we developed a systematic study of the annihilation field that is determined from the maximum of the derivative dM/dB in the increasing magnetization branch of the hysteresis loop, which corresponds to the expulsion of the vortex core. All hysteresis curves were obtained starting from the unperturbed configuration obtained by minimizing the energy of the disks $B = 0$, which corresponds to the vortex core at the center. In sequence, we increase the field from $B = 0$, in steps of $\Delta B = 0.1$ mT, leading us to obtain the annihilation field, and finally reaching the magnetic saturation. In some simulations, we observed a deformation of the vortex core. In order to characterize it, we define

$$\delta = \frac{r_y - r_x}{r_x}, \tag{1}$$

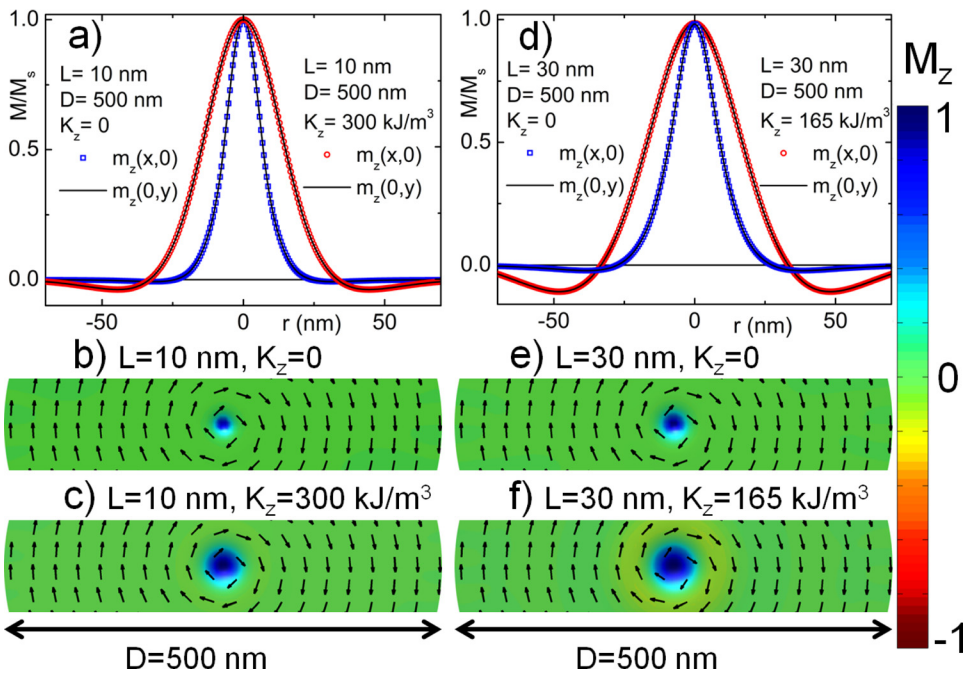

FIG. 1. (a) Profile of the vortex core corresponding to disks with $D = 500$ nm and $L = 10$ nm for $K_z = 0$ and $K_z = 300$ kJ/m^3; (b) and (c) depict the magnetization for $K_z = 0$ and $K_z = 300$ kJ/m^3 with $L = 10$ nm. (d) Profile of the vortex core with $D = 500$ nm and $L = 30$ nm for $K_z = 0$ and $K_z = 165$ kJ/m^3. (e) and (f) represent the magnetization for $K_z = 0$ and $K_z = 165$ kJ/m^3 for $L = 30$ nm. Note that from (a) to (d) the depth of the negative part of the magnetization (the dip) increases.

where r_x and r_y are the sizes of the vortex core along the x and y axes, respectively. As shown in Fig. 1, two orthogonal sections (x and y directions) of the profiles of the vortex core passing through the core center (maximum of m_z) were obtained. The dimensions of the core along the x and y directions were obtained by the full widths at half maximum of the respective profile fit, using a pseudo-Voigt function.

III. ANALYTICAL MODEL

To obtain analytical expressions for the annihilation field in the magnetic nanodots, we started with a model proposed by Guslienko *et al.*[20,21] to investigate the vortex behavior in submicron dots. These authors considered a ferromagnetic dot with a thickness L and a radius R that presents a vortex state with a distribution of the unit magnetization in cylindrical coordinates ρ, φ, z given by $\vec{m} = \sin\theta(\rho)\hat{\phi} + \cos\theta(\rho)\hat{z}$, where[21]

$$m_\phi = \sin\theta(\rho) = \begin{cases} (2b\rho/(b^2+\rho^2)) & \rho \le b \\ 1 & \rho \ge b. \end{cases} \quad (2)$$

Here b is the radius of the core. If we consider magnetostatic, exchange, and Zeeman contributions to the energy, the normalized dimensionless vortex annihilation field in the rigid core model proposed by Guslienko *et al.*[21] is written as

$$h_{an}(\beta, R) = 4\pi F_1(\beta) - \left(\frac{R_0}{R}\right)^2, \quad (3)$$

where $\beta = L/R$, R_0 is the exchange length and $F_1(\beta)$ is given by

$$F_1(\beta, R) = \int_0^\infty \left(1 - \frac{1-e^{-\beta t}}{\beta t}\right) J_1^2(t)\frac{dt}{t}. \quad (4)$$

A. Introducing a perpendicular uniaxial anisotropy

While the model proposed by Guslienko *et al.*[20,21] contains no anisotropy, in our calculations we include a uniaxial anisotropy along the z axis and focus on its effect on the annihilation field. We start calculating the anisotropy energy contribution of the system that is given by

$$W_K = -LK_z \int (\vec{m}\cdot\hat{z})^2 \rho d\phi d\rho, \quad (5)$$

where $K_z > 0$ is the anisotropy constant and $\hat{z}$ is the easy axis. From this expression, the contribution to the energy of the core due to the anisotropy comes only from the core region inside the dot. From Fig. 2, we obtain

$$\phi_m = \arccos\left(\frac{x^2 + b^2 - R^2}{2xb}\right), \quad (6)$$

and

$$\rho_m = x\cos\phi + \sqrt{R^2 - x^2 + x^2\cos^2\phi}. \quad (7)$$

Using these expressions, we can write Eq. (5) as

$$W_K = -2K_zL\int_0^{\phi_m}\left[\int_0^b m_z^2 \rho d\rho\right]d\phi - 2K_zL\int_{\phi_m}^{\pi}\left[\int_0^{\rho_m} m_z^2 \rho d\rho\right]d\phi, \quad (8)$$

$$W_K = -K_zLb^2\sec^{-1}\left[\frac{2bx}{b^2 - R^2 + x^2}\right](3 - 2\ln 4) - G. \quad (9)$$

In this expression, $m_z^2 = \left(1 - 4b^2\rho^2/(b^2+\rho^2)^2\right)$ and G represents the contributions to the anisotropy energy shown in the dark regions in Fig. 2(a),

$$G = 2K_zL\int_{\phi_m}^{\pi}\left[\int_0^{\rho_m}\left(1 - \frac{4b^2\rho^2}{(b^2+\rho^2)^2}\right)\rho\, d\rho\right]d\phi. \quad (10)$$

When $\phi_m(x \to R) \approx \pi/2$ or $c = b/R \ll 1$, G can be approximated to zero at first order of $(R - x)$. However, in our calculations we considered it explicitly. If the anisotropy energy is normalized to M_s^2V, that is, $w_K = W_K/(M_s^2V)$, and using $s = x/R$, $c = b/R$, and $V = \pi R^2 L$, we obtain

$$w_K(s) = \frac{-K_zc^2}{\pi M_s^2}\sec^{-1}\left[\frac{2cs}{c^2 - 1 + s^2}\right](3 - 2\ln 4) - g(s), \quad (11)$$

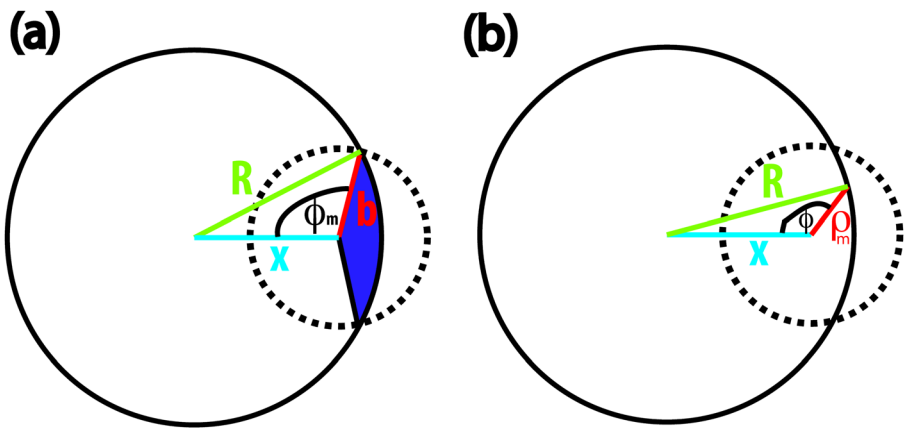

FIG. 2. Geometrical relation between the vortex core, defined by the dotted line, and the full dot. (a) Illustration of the angle ϕ_m that depends on the radius of the dot, R, radius of the core, b, and separation between the centers of the dot and core, x. (b) Representation of ρ_m that depends on R, x, and the angle ϕ between x and ρ_m.

where $g(s) = G/M_s^2 V$. We proceed by minimizing the magnetic anisotropy energy with respect to s and evaluating in the equilibrium displacement where the vortex center reaches the dot perimeter. In other words, differentiating Eq. (11) with respect to s and taking the limit $s \to 1$, we obtain the value of the contribution of the anisotropy to the annihilation field

$$h_K = \lim_{s\to 1} \frac{\partial w_K(s)}{\partial s} = -\frac{K_z}{M_s^2} \frac{c(c^2-2)(\ln 16 - 3)}{\pi\sqrt{4-c^2}} - \lim_{s\to 1} \frac{\partial g(s)}{\partial s}. \quad (12)$$

In this way, and adding this expression to the annihilation field given by Eq. (3), we obtain the annihilation field for a nanodot with perpendicular anisotropy,

$$h_{an}(\beta, R) = 4\pi F_1(\beta) - \left(\frac{R_0}{R}\right)^2 - \frac{K_z}{M_s^2} \frac{c(c^2-2)(-3+\ln 16)}{\pi\sqrt{4-c^2}} - \lim_{s\to 1} \frac{\partial g(s)}{\partial s}. \quad (13)$$

IV. RESULTS AND DISCUSSION

Our analyses for the annihilation field are based on the theoretical approach and on micromagnetic simulations. From both approaches, we have obtained the dependence of the annihilation fields with the perpendicular anisotropy. Also from the simulations, we obtained the evolution of the magnetic core shape while it moves along the dot.

A. Annihilation fields

The annihilation fields as a function of the disk diameter, for different anisotropies K_z, obtained from both methods are reported in Figs. 3–5 for $L = 10$, 20, and 30 nm, respectively. From those figures, we observe that the two approaches evidence a qualitative agreement, showing that as the diameter of the disks increases, B_{an} decreases and becomes less dependent on the anisotropy. However, in spite of the fact that they have the same magnitude, the analytical calculations result in larger (≈20%) annihilation fields as compared to the numerical simulations. A maximum of the curves appears from the micromagnetic simulations that is not evidenced in the analytical model.

The existence of these maxima, previously reported by Guslienko *et al.* for non-anisotropic materials,[20] can be qualitatively understood by looking into the different contributions

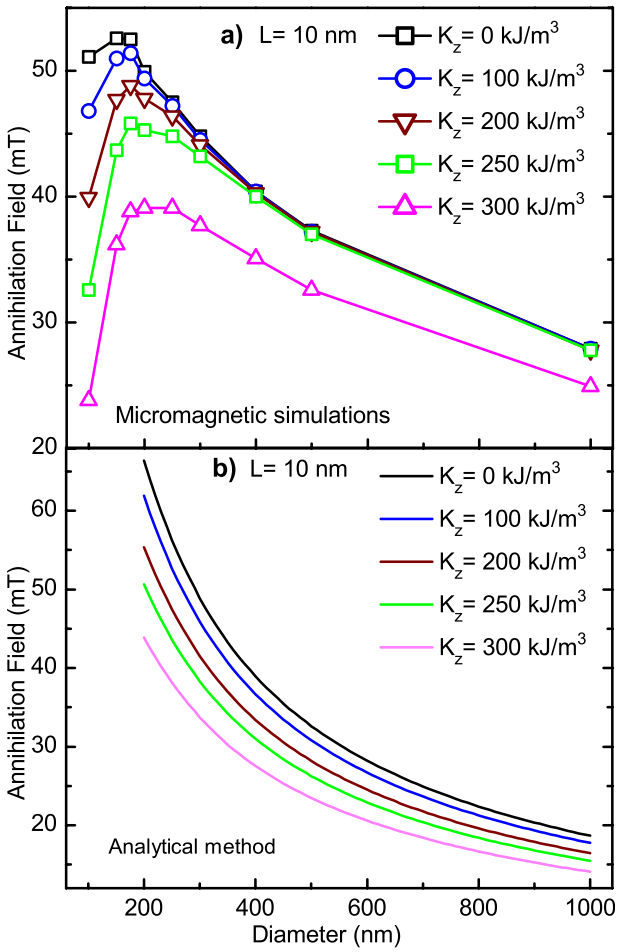

FIG. 3. Annihilation fields versus diameter for dots (a) obtained by micromagnetic simulation, and (b) obtained by analytical method. These graphs show the influence of the value of the perpendicular anisotropy on the annihilation field for different diameters.

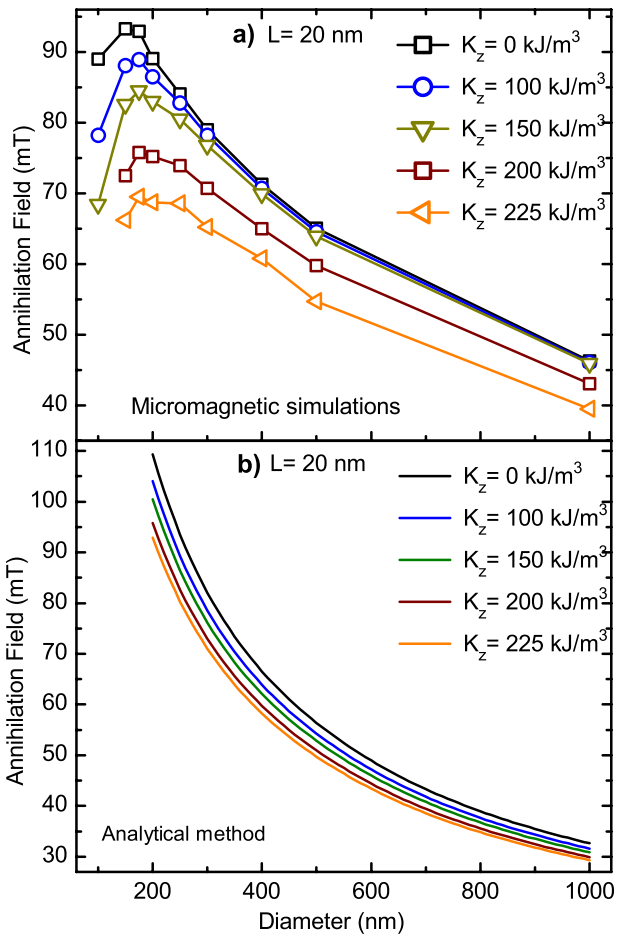

FIG. 4. Annihilation fields versus diameter for dots (a) obtained by numerical calculation and (b) obtained by the analytical method.

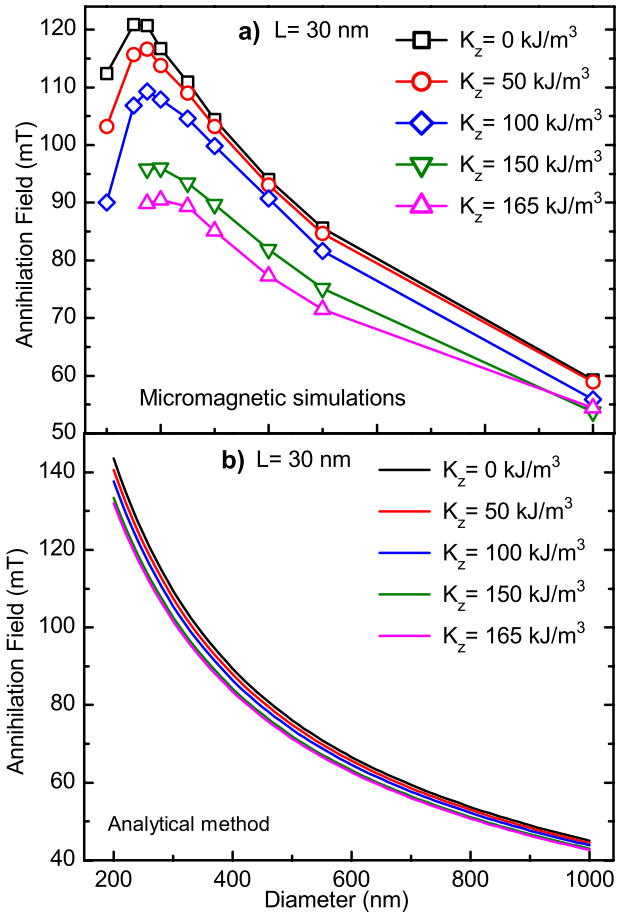

FIG. 5. Annihilation fields versus diameter for dots with (a) and obtained by numerical calculation and (b) obtained by the analytical method.

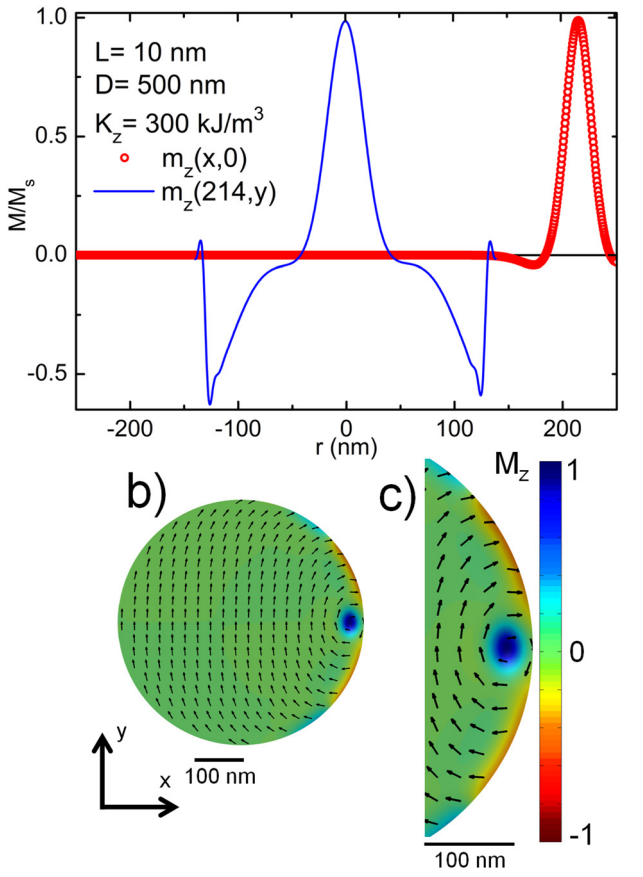

FIG. 6. Shape of the vortex core for $L = 10\,\text{nm}$, $D = 500\,\text{nm}$, and $K_z = 300\,\text{kJ/m}^3$ immediately before the annihilation. (a) Profile of the core along the x axis (red dotted line) and along the y axis (blue continuous line). (b) Representation of the disk. (c) A detail of the disk section close to the vortex core.

to the energy. In the presence of a vortex at the center of the dot, an important contribution to the energy comes from the core. If this core is small compared to the dot radius, its contribution to the total energy is small, but if it is large compared to the size of the dot, its energy contribution will be important. In this case, the system will decrease its energy by moving fast the core to one extreme, leading to a decrease of the annihilation field. Since the size of the core is independent of the dot diameter,[33] this will occur at some specific diameter for each thickness, leading to a particular value for the maximum for each thickness.

From the simulations, we also observe that larger anisotropies result in larger core sizes, as shown in Fig. 1. The disagreement between the two methods can be related to a deformation of the core observed in the micromagnetic simulations, as shown in Sec. IV B. In addition, in our analytical results we considered only first order terms on s for the energy contributions and we overestimate the magnetostatic energy, generating differences between simulations and analytical calculations for small radii.[21] This was previously reported by Guslienko *et al.*[20] who stated that the rigid core model overestimates the magnetostatic energy, leading to differences between theory and simulations that are more evident for small R, where the model includes larger magnetostatic terms.

B. Evolution of the magnetic core shape

In the search for an explanation of the differences between B_{an} derived by the analytical method and by numerical calculation, we studied the shape of the core. From our micromagnetic simulations, we obtained the shape of the magnetic vortex core as it moves towards the edge of the disk under the influence of an applied magnetic field for the maximum anisotropies, $K_z^{max} = 300$ and $165\,\text{kJ/m}^3$ for $L = 10\,\text{nm}$ and $L = 30\,\text{nm}$, respectively. Our results, for $D = 500\,\text{nm}$ dots, are depicted in Figs. 6 and 7. The dark region (blue online) in these figures represents the core region. The profile of the vortex core at the center of the disk is shown in Fig. 1. By comparing these results with the ones presented in Fig. 1, a gradual deformation of the vortex core is evidenced, exhibiting a nearly elliptical ("banana-like") shape while reaching the edge of the dot. Comparing Fig. 1 and Figs. 6 and 7, we can conclude that the core is circular at the center of the disk and for $B = 0$; the deformation is maximum when the core reaches the edge of the disk, immediately before the vortex annihilation. In Fig. 7(b) for a thicker disk, the core and its deformation are enhanced. As the core reaches the disk edge (y-axis), the xy symmetry is broken; a core with circular section would increase the magnetic charges on the edge, and the appearance of the deformation following the edge surface reduces the stray fields.

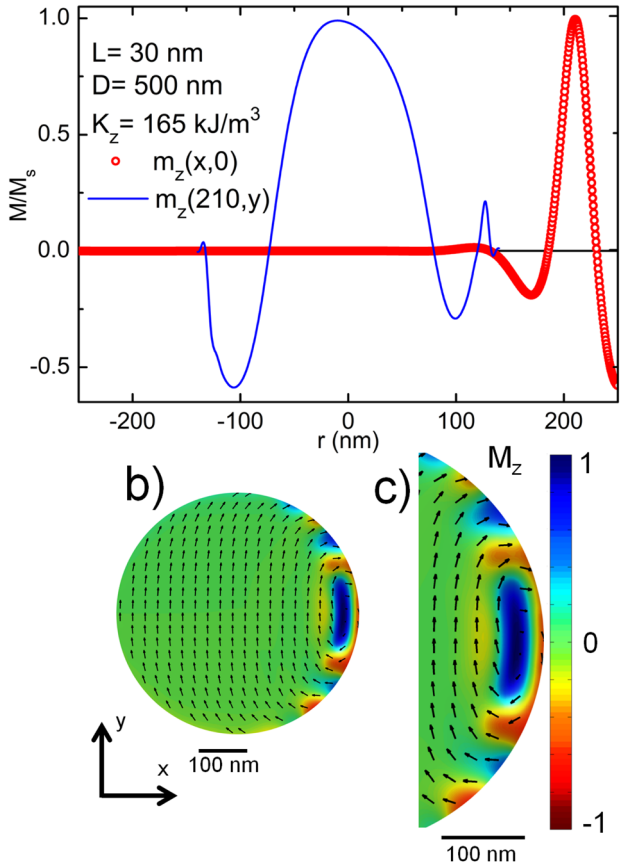

FIG. 7. Change of the shape of the vortex core for $L = 30$ nm, $D = 500$ nm, and $K_z = 165$ kJ/m^3 at positions immediately before annihilation. In (a) profile of the core along the x axis (red dotted line) and along the y axis (blue continuous line), in (b) image of the disk and (c) a detail of the disk.

This effect has not been considered in developing the rigid vortex mode, that breaks down in the cases where important deformations of the vortex core are observed.

For $L = 10$ nm, the core keeps a nearly circular shape with a deformation δ of about 10% for zero anisotropy ($K_z = 0$), and around 30% for $K_z = 300$ kJ/m^3. By comparing

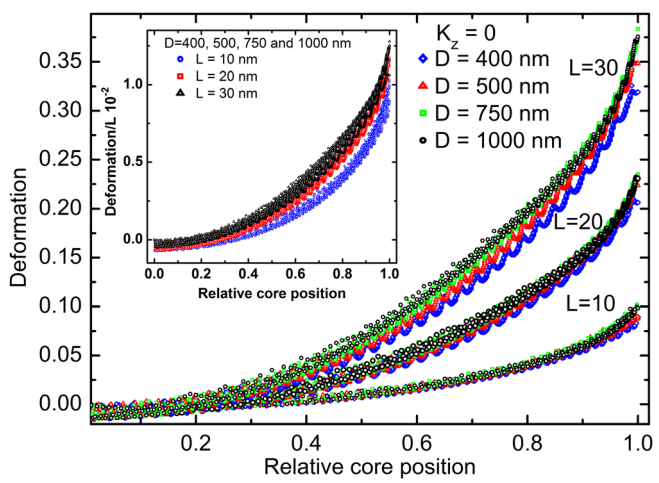

FIG. 8. Deformation $\delta = (r_y - r_x)/r_x$ for $K_z = 0$ kJ/m^3, $L = 10$, 20, and 30 nm for diameters $D = 400$, 500, 750, and 1000 nm versus normalized core position (P_{core}/R). The inset shows the deformation divided by the disk thickness, for different values of L, versus relative core positions. Note that a scaling law is apparent.

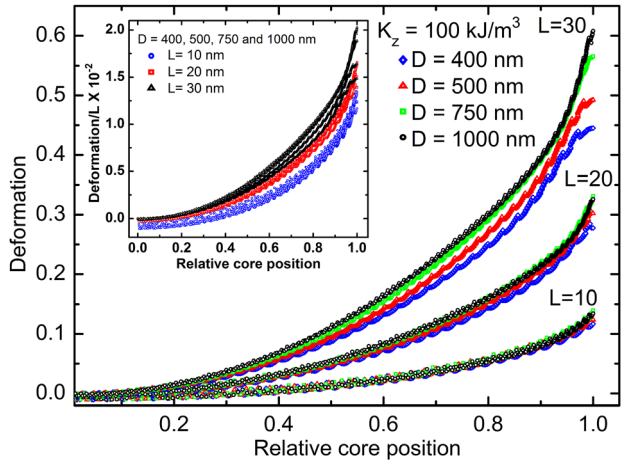

FIG. 9. Deformation $\delta = (r_y - r_x)/r_x$ for $K_z = 100$ kJ/m^3, $L = 10$, 20, and 30 nm for diameters $D = 400$, 500, 750, and 1000 nm versus normalized core position (Pcore/R). The inset shows the deformation divided by the disk thickness, for different values of L, versus relative core positions. Note that a scaling law is apparent.

Figs. 1(a)–1(c) with Fig. 6, we observe that the vortex core deformation is due to an increase of its size along the y axis and the depth of the magnetization dip. For thicker dots, i.e., $L = 30$ nm, the smallest core deformation is $\delta = 30\%$ for $K_z = 0$, and around 100% for $K_z = 165$ kJ/m^3. Therefore, larger anisotropies increase the vortex core deformation, leading to a core of roughly elliptical section that is not well described by the rigid vortex model. This is shown in Figs. 6 and 7, where it is more evident the deformation of the vortex core, as well as the variation in the magnetization dip. It is important to note that an anisotropy constant higher than $K_z = 165$ kJ/m^3 for $L = 30$ nm is not compatible with a vortex configuration, as mentioned above.

To investigate the deformation process in a systematic way, we obtained the deformation δ versus the normalized core position, P_{core}/R, where P_{core} is the distance of the core center measured from the center of the disk, divided by the disk radius (R). Our results are depicted in Figs. 8 and 9, evidencing that the core deformation is not present for $\mathbf{B} = \mathbf{0}$, however, as the field begins to increase, the process of deformation of the core sets in. When P_{core} is less than 0.25, the deformation of the core can be neglected. From this position onwards the deformation begins to increase, and the maximum is reached when the core approaches the edge of the disk. Note that in Figs. 8 and 9 for each thickness (10, 20, and 30 nm) four curves were plotted for different diameters (400, 500, 750, and 1000 nm). The inset illustrates a normalized deformation, that is δ/L, showing a scaling law for the deformation of the core. The oscillations superposed on the curves are artifacts arising from the finite size of the cells.

V. CONCLUSIONS

In summary, by means of an analytical model and numerical simulations we have obtained the annihilation fields for dots of different thicknesses and anisotropy constants. In all cases, the annihilation fields decrease with increasing anisotropy constant K_z and with increasing disk diameter, D. The values of K_z and disk thickness L have a stronger effect

on the annihilation fields of the smaller disks. However, they influence in an inverse way the annihilation field; whereas the increase in thickness increases the annihilation field, from the analytical results using the rigid vortex model, the increase in anisotropy decreases this field. Finally, we have shown the variation in the deformation of the vortex core δ as a function of the perpendicular anisotropy and disk thickness. The occurrence of this deformation evidenced in the micromagnetic simulations suggests that it has to be taken into account in the description of the dynamics of the magnetic vortices. The deformation of the core does not scale with the radius of the disks, it is only related to the relative position of the core.

ACKNOWLEDGMENTS

In Brazil we acknowledge the support of the agencies CAPES, CNPq, FAPERJ and FAPESP. In Chile, we acknowledge the partial support from FONDECYT under Grant Nos. 11121214, 1120356, and 1120618, from the Center for the Development of Nanoscience and Nanotechnology, and from ICM P10-06-F funded by Fondo de Innovación para la Competitividad, from the MINECON, and CONICYT-PAI/CONCURSO INSERCIÓN EN LA ACADEMIA-FOLIO 791220017.

[1]A. P. Guimarães, *Principles of Nanomagnetism* (Springer, Berlin, 2009).
[2]C. L. Chien, F. Q. Zhu, and J.-G. Zhu, Phys. Today **60**(6), 40 (2007).
[3]K. Y. Guslienko, J. Nanosci. Nanotechnol. **8**, 2745 (2008).
[4]S. Bohlens, B. Kruger, A. Drews, M. Bolte, G. Meier, and D. Pfannkuche, Appl. Phys. Lett. **93**, 142508 (2008).
[5]A. Ruotolo, V. Cros, B. Georges, A. Dussaux, J. Grollier, C. Deranlot, R. Guillemet, K. Bouzehouane, S. Fusil, and A. Fert, Nat. Nanotechnol. **4**, 528 (2009).
[6]H. Jung, Y.-S. Choi, K.-S. Lee, D.-S. Han, Y.-S. Yu, M.-Y. Im, P. Fischer, and S.-K. Kim, ACS Nano **6**, 3712 (2012), http://pubs.acs.org/doi/pdf/10.1021/nn3000143.
[7]M. Bode, O. Pietzsch, A. Kubetzka, W. Wulfhekel, D. McGrouther, S. McVitie, and J. N. Chapman, Phys. Rev. Lett. **100**, 029703 (2008).
[8]P. Landeros, J. Escrig, D. Altbir, D. Laroze, J. d'Albuquerque e Castro, and P. Vargas, Phys. Rev. B **71**, 094435 (2005).
[9]D. Altbir, J. Escrig, P. Landeros, F. S. Amaral, and M. Bahiana, Nanotechnology **18**, 485707 (2007).
[10]W. Zhang, R. Singh, N. Bray-Ali, and S. Haas, Phys. Rev. B **77**, 144428 (2008).
[11]K. L. Metlov and Y. Lee, Appl. Phys. Lett. **92**, 112506 (2008).
[12]M. M. Soares, E. de Biasi, L. N. Coelho, M. C. dos Santos, F. S. de Menezes, M. Knobel, L. C. Sampaio, and F. Garcia, Phys. Rev. B **77**, 224405 (2008).
[13]S.-H. Chung, R. D. McMichael, D. T. Pierce, and J. Unguris, Phys. Rev. B **81**, 024410 (2010).
[14]E. R. P. Novais, P. Landeros, A. G. S. Barbosa, M. D. Martins, F. Garcia, and A. P. Guimarães, J. Appl. Phys **110**, 053917 (2011).
[15]M. Rahm, M. Schneider, J. Biberger, R. Pulwey, J. Zweck, D. Weiss, and V. Umansky, Appl. Phys. Lett. **82**, 4110 (2003).
[16]S.-K. Kim, K.-S. Lee, Y.-S. Yu, and Y.-S. Choi, Appl. Phys. Lett. **92**, 022509 (2008).
[17]F. Garcia, H. Westfahl, J. Schoenmaker, E. J. Carvalho, A. D. Santos, M. Pojar, A. C. Seabra, R. Belkhou, A. Bendounan, E. R. P. Novais, and A. P. Guimarães, Appl. Phys. Lett. **97**, 022501 (2010).
[18]M. Schneider, H. Hoffmann, and J. Zweck, Appl. Phys. Lett. **77**, 2909 (2000).
[19]A. Fernandez and C. J. Cerjan, J. Appl. Phys **87**, 1395 (2000).
[20]K. Y. Guslienko and K. L. Metlov, Phys. Rev. B **63**, 100403 (2001).
[21]K. Y. Guslienko, V. Novosad, Y. Otani, H. Shima, and K. Fukamichi, Phys. Rev. B **65**, 024414 (2001).
[22]J. Mejia-Lopez, D. Altbir, A. H. Romero, X. Batlle, I. V. Roshchin, C.-P. Li, and I. K. Schuller, J. Appl. Phys **100**, 104319 (2006).
[23]J. Mejía-López, D. Altbir, P. Landeros, J. Escrig, A. H. Romero, I. V. Roshchin, C.-P. Li, M. R. Fitzsimmons, X. Batlle, and I. K. Schuller, Phys. Rev. B **81**, 184417 (2010).
[24]K.-M. Wu, L. Horng, J.-F. Wang, J.-C. Wu, Y.-H. Wu, and C.-M. Lee, Appl. Phys. Lett. **92**, 262507 (2008).
[25]R. K. Dumas, T. Gredig, C.-P. Li, I. K. Schuller, and K. Liu, Phys. Rev. B **80**, 014416 (2009).
[26]G. Mihajlović, M. S. Patrick, J. E. Pearson, V. Novosad, S. D. Bader, M. Field, G. J. Sullivan, and A. Hoffmann, Appl. Phys. Lett. **96**, 112501 (2010).
[27]J. P. Davis, D. Vick, J. A. J. Burgess, D. C. Fortin, P. Li, V. Sauer, W. K. Hiebert, and M. R. Freeman, New J. Phys. **12**, 093033 (2010).
[28]T. S. Machado, T. G. Rappoport, and L. C. Sampaio, Appl. Phys. Lett. **93**, 112507 (2008).
[29]A. Fert, V. Cros, and J. Sampaio, Nat. Nanotechnol. **8**, 152 (2013).
[30]X. Z. Yu, Y. Onose, N. Kanazawa, J. H. Park, J. H. Han, Y. Matsui, N. Nagaosa, and Y. Tokura, Nature **465**, 901–904 (2010).
[31]S.-K. Kim, J. Phys. D: Appl. Phys **43**, 264004 (2010).
[32]M. Donahue and D. Porter, *Oommf User's guide* (NIST, 1999).
[33]T. Shinjo, T. Okuno, R. Hassdorf, K. Shigeto, and T. Ono, Science **289**, 930 (2000).